Human CHCHD4 mitochondrial proteins regulate cellular oxygen consumption rate and metabolism and provide a critical role in hypoxia signaling and tumor progression

Jun Yang,[1] Oliver Staples,[1] Luke W. Thomas,[1] Thomas Briston,[1] Mathew Robson,[2] Evon Poon,[1] Maria L. Simões,[1] Ethaar El-Emir,[2] Francesca M. Buffa,[3] Afshan Ahmed,[1] Nicholas P. Annear,[1] Deepa Shukla,[1] Barbara R. Pedley,[2] Patrick H. Maxwell,[1,4] Adrian L. Harris,[3] and Margaret Ashcroft[1]

[1]Centre for Cell Signalling and Molecular Genetics, University College London, Division of Medicine, Rayne Institute, London, United Kingdom. [2]Tumour Biology Section, UCL Cancer Institute, Paul O'Gorman Building, University College London, London, United Kingdom. [3]Cancer Research UK Department of Medical Oncology, The Weatherall Institute of Molecular Medicine, University of Oxford, John Radcliffe Hospital, Oxford, United Kingdom. [4]Faculty of Medical Sciences, University College London, Division of Medicine, Rayne Institute, London, United Kingdom.

Increased expression of the regulatory subunit of HIFs (HIF-1α or HIF-2α) is associated with metabolic adaptation, angiogenesis, and tumor progression. Understanding how HIFs are regulated is of intense interest. Intriguingly, the molecular mechanisms that link mitochondrial function with the HIF-regulated response to hypoxia remain to be unraveled. Here we describe what we believe to be novel functions of the human gene *CHCHD4* in this context. We found that *CHCHD4* encodes 2 alternatively spliced, differentially expressed isoforms (CHCHD4.1 and CHCHD4.2). CHCHD4.1 is identical to MIA40, the homolog of yeast Mia40, a key component of the mitochondrial disulfide relay system that regulates electron transfer to cytochrome *c*. Further analysis revealed that CHCHD4 proteins contain an evolutionarily conserved coiled-coil-helix-coiled-coil-helix (CHCH) domain important for mitochondrial localization. Modulation of CHCHD4 protein expression in tumor cells regulated cellular oxygen consumption rate and metabolism. Targeting *CHCHD4* expression blocked HIF-1α induction and function in hypoxia and resulted in inhibition of tumor growth and angiogenesis in vivo. Overexpression of CHCHD4 proteins in tumor cells enhanced HIF-1α protein stabilization in hypoxic conditions, an effect insensitive to antioxidant treatment. In human cancers, increased *CHCHD4* expression was found to correlate with the hypoxia gene expression signature, increasing tumor grade, and reduced patient survival. Thus, our study identifies a mitochondrial mechanism that is critical for regulating the hypoxic response in tumors.

Introduction

The HIF pathway plays a central role in both sensing and responding to changes in cellular oxygen levels (1). HIFs (HIF-1 or HIF-2) are basic helix-loop-helix/per/arnt/sim domain (bHLH/PAS) transcription factors, composed of a regulatory HIF-α subunit (HIF-1α or HIF-2α) and constitutively expressed β subunit (HIF-1β) (2). HIF-α is rapidly stabilized in response to hypoxia and, upon binding to HIF-1β in the nucleus, transactivates the expression of numerous genes involved in cellular processes, such as angiogenesis, metabolic adaptation, and cell survival. Increased expression of HIF-α is observed in many human cancers and usually correlates with increased vascular density, the severity of tumor grade, and a poor prognostic outcome using conventional treatments. Therefore, understanding how HIF-α becomes deregulated in cancer is particularly relevant to identifying new therapeutic strategies for targeting the HIF pathway (3).

During the last decade, great advances have been made in our understanding of HIF-α regulation by oxygen (1). HIF-α protein stability is tightly regulated by oxygen-dependent prolyl hydroxylase domain (PHD) enzymes (4–6). Prolyl hydroxylation of HIF-α leads to the recognition and binding of the von Hippel-Lindau (VHL) E3 ligase, which targets HIF-α for ubiquitin-mediated degradation via the proteasome (4, 5, 7). Of particular interest are previous studies indicating that mitochondria are important for HIF-1α induction and HIF-1–dependent gene transcription in response to hypoxia (8–14). Reactive oxygen species (ROS) released from complex III in response to hypoxia are proposed to play a role in the stabilization of HIF-1α (9, 11, 13) by inhibiting PHD-mediated hydroxylation of HIF-1α (15). Pharmacological inhibitors of the respiratory chain reaction, loss of cytochrome *c*, or genetic knockdown of mitochondrial complex components suppress hypoxia-induced ROS production and HIF-1α stabilization (11, 13, 16). In addition, alterations in mitochondrial oxygen consumption via cytochrome *c* oxidase (COX [complex IV]) have been proposed to regulate HIF-1α stabilization in a ROS-independent manner (10, 17–19).

The emerging relationship between mitochondria and components of the respiratory chain in oxygen sensing, HIF-α induction, and the hypoxic response suggests that novel molecular mechanisms exist to regulate HIF-α function and hypoxia signaling via the mitochondria. For the first time to our knowledge, here we describe a role for the CHCHD4 (also known as MIA40) mitochondrial proteins in HIF-1α regulation, metabolism, and tumor progression.

Authorship note: Jun Yang and Oliver Staples contributed equally to this work.
Conflict of interest: The authors have declared that no conflict of interest exists.
Citation for this article: *J Clin Invest.* 2012;122(2):600–611. doi:10.1172/JCI58780.

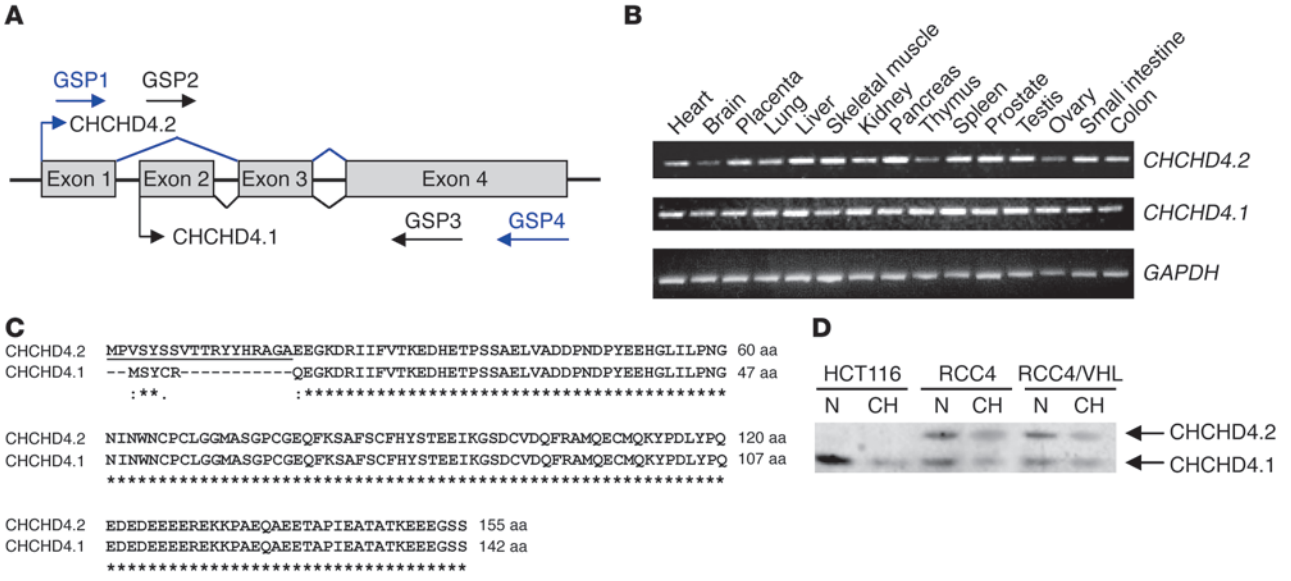

Figure 1

CHCHD4 encodes 2 alternatively spliced and differentially expressed isoforms. (**A**) Schematic representation of the *CHCHD4* genomic region showing 4 exons that are subject to alternative splicing. Exons are represented by gray boxes, introns are represented by black thick lines, and patterns of alternative splicing are represented by thin lines (blue and black). Gene-specific primers (GSP) were used for PCR to examine the alternative splicing transcripts. (**B**) Human tissue expression analysis shows that the *CHCHD4* transcripts are ubiquitously expressed. Gene-specific primers for *CHCHD4.1* and *CHCHD4.2* described in **A** were used to examine human tissue expression, as indicated by RT-PCR. *GAPDH* was used as a loading control. (**C**) The amino acid sequences encoded by CHCHD4.1 and CHCHD4.2 were aligned using the ClustalW program. The short N-terminal sequence in CHCHD4.2 is underlined. Identical (asterisk), conserved (double dot), and partially conserved (single dot) amino acid residues are indicated. (**D**) Western blot showing differential expression of the CHCHD4 proteins in tumor cells. HCT116, RCC4, and RCC4/VHL cells were transfected with CHCHD4 siRNA (CH) or NSC (N) siRNA. Cell lysates were analyzed by Western blot for endogenous CHCHD4 proteins (CHCHD4.1 and CHCHD4.2) as indicated (arrows).

Results

CHCHD4 encodes 2 alternatively spliced and differentially expressed isoforms. Using a bioinformatics approach that has been described previously (20–22), we performed analyses to identify protein regulators of HIF-1α (see Supplemental Methods; supplemental material available online with this article; doi:10.1172/JCI58780DS1). We identified *CHCHD4* transcript variant 2 (GenBank accession no. NM_144636.2, GI no. 148612891; http://www.ncbi.nlm.nih.gov/sites/entrez?db=nucleotide). The human *CHCHD4* gene is located on chromosome 3p25.1 and consists of 4 exons (GenBank accession no. BC033775, GeneID 131474). Using the BLAST homology search algorithm (http://www.ncbi.nlm.nih.gov/BLAST), we found that *CHCHD4* is predicted to generate 2 alternatively spliced mRNA transcripts termed *CHCHD4* transcript variant 1 (*CHCHD4.1*; GenBank accession no. NM_001098502, GI no. 148612858) and *CHCHD4* transcript variant 2 (*CHCHD4.2*; GenBank accession no. NM_144636.2, GI no. 148612891). *CHCHD4.1* encodes exon 2 to exon 4, while *CHCHD4.2* encodes exon 1, exon 3, and exon 4 (Figure 1A). To examine the expression pattern of the *CHCHD4* isoforms in different human tissues, we designed exon specific primers and determined their mRNA expression pattern using RT-PCR. We found that both *CHCHD4* isoforms were expressed across a variety of human tissues (Figure 1B). Interestingly, we found that *CHCHD4.2* displayed a differential expression pattern, while the expression levels of *CHCHD4.1* were found to be similar in all human tissues that we examined (Figure 1B).

Further analysis indicated that *CHCHD4.1* encodes a protein of 142 amino acids, CHCHD4.1, which is identical to MIA40 (23, 24), while *CHCHD4.2* contains an open reading frame encoding a protein of 155 amino acids, CHCHD4.2 (Figure 1C). Sequence comparison revealed that the 2 proteins only differ by a short additional N-terminal sequence found in CHCHD4.2 (Figure 1C). To assess the relative abundance of the CHCHD4 proteins, we examined a panel of human tumor cell lines, including HCT116 (colon carcinoma), MCF-7 (breast carcinoma), Saos-2 (osteosarcoma), and RCC4 (renal carcinoma) cells, using specific antibodies that recognize both protein isoforms. Consistent with our findings for the *CHCHD4* transcripts (Figure 1B), we found that CHCHD4.1 was the most abundant isoform detected (Figure 1D and Supplemental Figure 1), while CHCHD4.2 protein appeared to be differentially expressed (Figure 1D). We used short interfering RNA (siRNA) duplexes, designed to knock down the expression of both CHCHD4 proteins, to further confirm their expression in the cell lines used (Figure 1D and Supplemental Figure 1).

CHCHD4 proteins contain an evolutionarily conserved coiled-coil-helix-coiled-coil-helix domain and localize to mitochondria. Examination of the CHCHD4 proteins across species indicated that they share 6 highly evolutionarily conserved cysteines (Figure 2A), 4 of which are located within a conserved coiled-coil-helix-coiled-coil-helix (CHCH) domain containing a characteristic Cx_9C motif (ref. 25 and Figure 2A). Yeast Mia40 and several other CHCH-domain containing proteins have been identified as mitochondrial proteins (23). To evaluate the subcellular localization of endogenous and exogenously expressed CHCHD4 proteins, we performed immunostaining and subcellular fractionation analyses. We found that both exogenously and endogenously expressed CHCHD4 proteins were predomi-

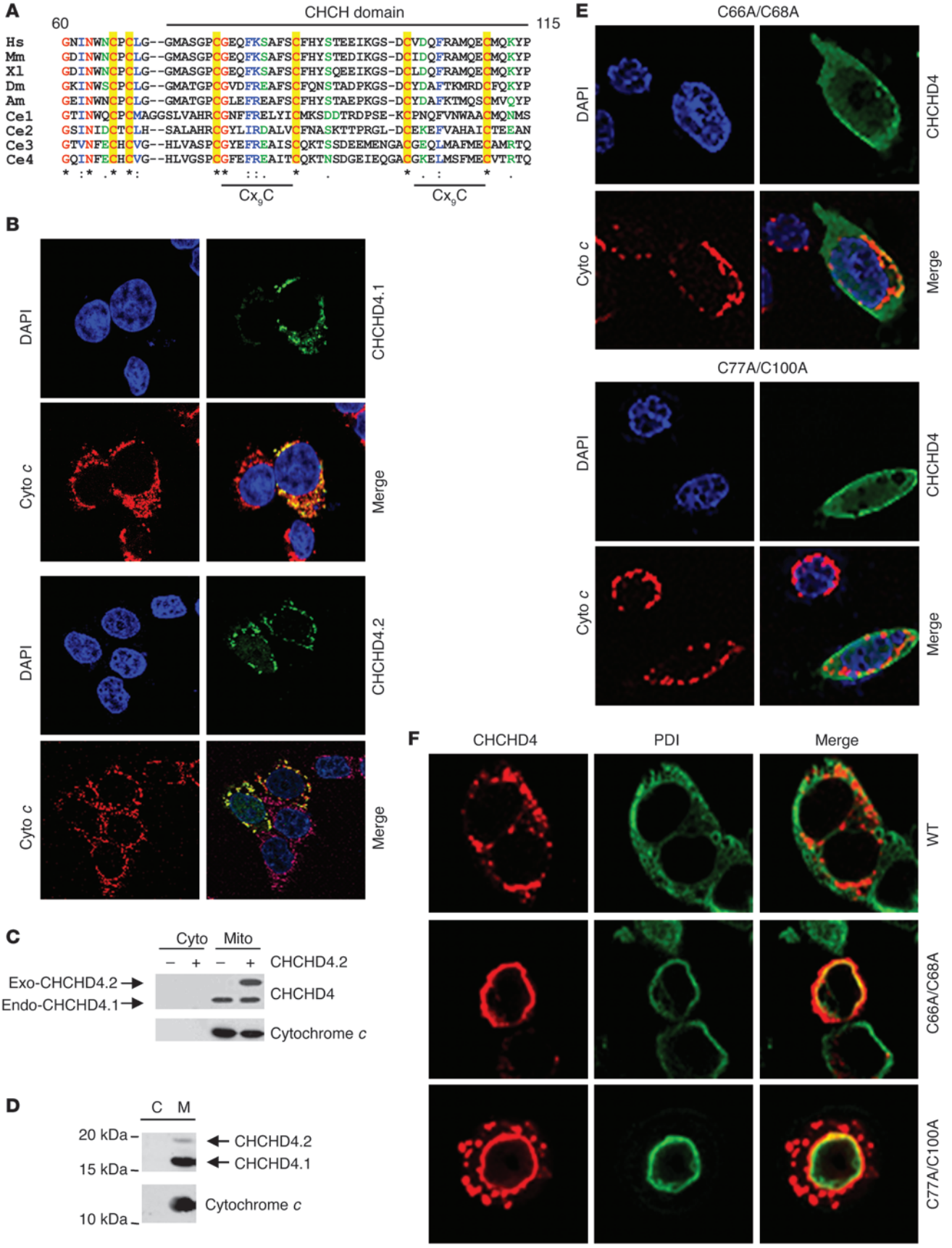
A
60
CHCH domain
115
Hs GNINWNCPCLG--GMASGPCGEQFKSAFSCFHYSTEEIKGS-DCVDQFRAMQECMQKYP
Mm GDINWNCPCLG--GMASGPCGEQFKSAFSCFHYSTEDIKGS-DCIDQFRAMQECMQKYP
Xl GDINWNCPCLG--GMASGPCGEQFKSAFSCFHYSQEEIKGS-DCLDQFRAMQECMQKYP
Dm GKINWSCPCLG--GMATGPCGVDFREAFSCFQNSTADPKGS-DCYDAFTKMRDCFQKYP
Am GEINWNCPCLG--GMATGPCGLEFREAFSCFHYSTAEPKGS-DCYDAFKTMQSCMVQYP
Ce1 GTINWQCPCMAGGSLVAHRCGNFFRELYICMKSDDTRDPSE-KCPNQFVNWAACMQNMS
Ce2 GSINIDCTCLH--SALAHRCGYLIRDALVCFNASKTTPRGL-DCEKEFVAHAICTEEAN
Ce3 GTVNFECHCVG--HLVASPCGYEFREAISCQKTSSDEEMENGACGEQLMAFMECAMRTQ
Ce4 GQINFECHCVG--HLVGSPCGFEFREAITCQKTNSDGEIEQGACGKELMSFMECVTRTQ
Cx9C
Cx9C
B
DAPI
CHCHD4.1
Cyto c
Merge
DAPI
CHCHD4.2
Cyto c
Merge
C
Cyto
Mito
– + – +
CHCHD4.2
Exo-CHCHD4.2
Endo-CHCHD4.1
CHCHD4
Cytochrome c
D
C M
20 kDa
15 kDa
10 kDa
CHCHD4.2
CHCHD4.1
Cytochrome c
E
C66A/C68A
DAPI
CHCHD4
Cyto c
Merge
C77A/C100A
DAPI
CHCHD4
Cyto c
Merge
F
CHCHD4
PDI
Merge
WT
C66A/C68A
C77A/C100A

Figure 2
CHCHD4 proteins contain an evolutionarily conserved CHCH domain and localize to mitochondria. (**A**) Sequence alignment of the CHCH domain of CHCHD4 and orthologs showing identical (red, asterisk), conserved (blue, double dot), and partially conserved (green, single dot) amino acid residues. The conserved 6 cysteine residues (red) are highlighted in yellow. The GEO accession numbers (http://www.ncbi.nlm.nih.gov/protein) are as follows: *H. sapiens* (Hm, NP_653237), *M. musculus* (Mm, NP_598689), *X. laevis* (Xl, AAH59772), *D. melanogaster* (Dm, AAN14214), *A. mellifera* (Am, XP_392382), *C. elegans* 1 (Ce1, NP_500803), *C. elegans* 2 (Ce2, NP_510159), *C. elegans* 3 (Ce3, NP_500804), and *C. elegans* 4 (Ce4, NP_498876). (**B**) Immunostaining analysis of HCT116 cells transfected with myc-tagged CHCHD4.1 or CHCHD4.2 expression vectors. Cells were fixed and stained with an anti-myc antibody (CHCHD4, green) and imaged by confocal microscopy. The mitochondria were visualized using an antibody to cytochrome *c* (red). The nuclei were stained with DAPI (blue). The overlay shows colocalized proteins in yellow. (**C**) Western blot showing endogenous and exogenously expressed CHCHD4 proteins in cytosolic (Cyto) and mitochondrial (Mito) fractions. Cytochrome *c* was used to confirm efficient mitochondrial fractionation. (**D**) Western blot analysis showing endogenous CHCHD4 proteins in HCT116 cells from cytosolic (C) and mitochondrial (M) fractions. Cytochrome *c* was used to confirm efficient mitochondrial fractionation. (**E** and **F**) Immunostaining analysis of HCT116 cells transfected with myc-tagged CHCHD4.2 cysteine mutants as indicated. Cells were fixed, stained, and imaged as described in **B**. (**F**) The ER was visualized using an antibody to PDI. The partial yellow staining in the overlay image indicates colocalization of CHCHD4.2 with PDI. Original magnification, ×60 (**B**); ×100 (**E** and **F**).

nantly localized to the mitochondria and colocalized with cytochrome *c* (Figure 2, B–D). Furthermore, we found that CHCHD4 proteins from isolated mitochondria were resistant to proteinase K treatment (Supplemental Figure 2A), confirming their localization to within mitochondria. Some mitochondrial proteins (e.g., Bax and Bak) can also localize to other subcellular compartments, such as the ER (26). Thus, using the specific ER marker protein disulfide isomerase (PDI) and the Golgi marker Golgin97, we assessed whether the CHCHD4 proteins localized elsewhere. We found that the CHCHD4 proteins were not detected in either ER, Golgi, or nuclear compartments (Supplemental Figure 2B and Supplemental Figure 3). To examine whether the highly conserved cysteines are important for subcellular localization of CHCHD4, we assessed the localization of cysteine-to-alanine substituted mutant proteins by immunofluorescence (Figure 2, E and F). Interestingly, we found that the highly conserved cysteines, including those within the CHCH domain, were important for CHCHD4 localization to mitochondria, since the CHCHD4-cysteine mutant proteins displayed a diffuse distribution in the cytoplasm (Figure 2E) and showed some partial localization to the ER (Figure 2F). Collectively, our data indicate that the CHCHD4 proteins are mitochondrial and that the highly evolutionarily conserved cysteines are important for regulating subcellular localization to mitochondria.

CHCHD4 proteins control cellular oxygen consumption rate and metabolism. Recent studies in yeast have identified Mia40 as a critical component of the mitochondrial disulfide relay system (DRS). Mia40, along with Erv1 of the DRS, participates in the transfer of electrons to molecular oxygen through interactions with cytochrome *c* and cytochrome *c* oxidase (COX, complex IV of the respiratory chain), thus linking the DRS to cytochrome *c* and the respiratory chain (27, 28). COX (complex IV) is an important site for regulating mitochondrial oxygen consumption rate (OCR) (29). Therefore, next we investigated whether CHCHD4 proteins regulate basal OCR and cellular ATP levels. Indeed, we found that overexpression of CHCHD4 enhanced basal OCR in HCT116 cells (Figure 3A and Supplemental Figure 4) and cellular ATP levels (Figure 3B). Conversely, we found that knockdown of CHCHD4 significantly reduced basal OCR (Figure 3A and Supplemental Figure 4) and cellular ATP levels, without affecting cytochrome *c* protein expression (Figure 3C). The significant reduction in basal OCR observed upon CHCHD4 knockdown is consistent with inhibitory effects observed using specific electron transport chain inhibitors (19).

CHCHD4 proteins are critical for HIF-1α induction and function in response to hypoxia. Given that CHCHD4 controls basal OCR (Figure 3), and intracellular oxygen levels tightly control HIF-1α protein availability (10), we hypothesized that CHCHD4 proteins may be important for regulating HIF-1α protein induction in response to hypoxia. We found that CHCHD4 knockdown inhibited HIF-1α protein induced in response to hypoxia in several cell lines (Figure 4A and Supplemental Figure 1), without affecting *Hif1a* mRNA levels (Supplemental Figure 5). Notably, we found that the subcellular localization and expression of the CHCHD4 proteins were the same in normoxia and hypoxia (Supplemental Figure 3). Interestingly, CHCHD4 knockdown did not significantly affect HIF-1α induced in response to deferoxamine mesylate (DFX) (Supplemental Figure 1A). Similar observations were described previously for cytochrome *c*–null mouse embryonic cells, in which loss of cytochrome *c* significantly reduced HIF-α induced in hypoxia but had no significant effect on DFX-induced HIF-α (13). Next, we examined whether CHCHD4 knockdown also affected HIF transcriptional activity. We found that the induction of GLUT-1, VEGF, and lysyl oxidase (LOX), the products of 3 known HIF target genes, was markedly reduced in hypoxia when CHCHD4 was knocked down (Figure 4, B–D). To examine whether the CHCHD4 proteins also regulate cell motility and invasion, we performed migration and invasion assays (Figure 4, E–G). We found that knockdown of either HIF-1α or CHCHD4 in several cell lines, including HCT116, resulted in a significant reduction in tumor cell migration (Figure 4E and Supplemental Figure 6), motility (Figure 4F), and invasion (Figure 4G). Our data indicate that CHCHD4 proteins can regulate HIF-1α induction and function in response to hypoxia in tumor cells.

Targeting CHCHD4 inhibits tumor growth and angiogenesis in vivo. To investigate the role of CHCHD4 in tumor growth and angiogenesis in vivo, we generated stable HCT116 cells expressing either 2 independent shRNA control vectors or 2 independent shRNA vectors designed to target *CHCHD4*. We found that targeting *CHCHD4* by shRNA blocked HIF-1α protein induction and CHCHD4 protein levels (Figure 5A) and significantly inhibited VEGF expression (Figure 5B) in response to hypoxia. We found that CHCHD4 knockdown had no significant effect on tumor cell proliferation in vitro (Figure 5C), although *Mia40* has been described as an essential gene in yeast (30, 31). Targeting *CHCHD4* by shRNA resulted in reduced tumor growth in vivo compared with that of independent tumors expressing 2 different shRNA controls (Figure 5D). Furthermore, using immunohistochemical analyses, we observed significantly reduced tumor blood vessel formation in the CHCHD4 shRNA knockdown tumor xenografts compared with that in tumors expressing the shRNA control (Figure 5, E and F). As anticipated, we found reduced nuclear HIF-1α expression immediately adjacent to the hypoxic regions within the tumor (as indicated by pimonidazole staining) and decreased expression

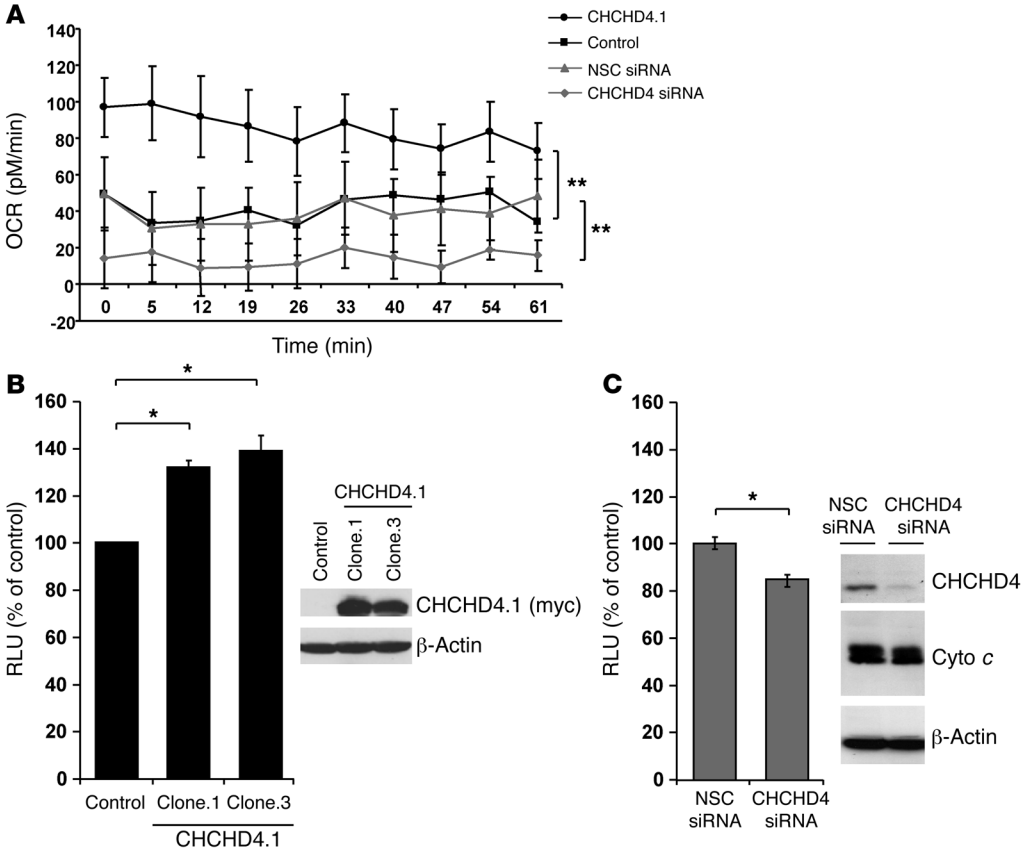

Figure 3

CHCHD4 proteins regulate basal cellular OCR and cellular ATP levels. CHCHD4.1 (myc-tagged), a control vector, CHCHD4 siRNA, or a NSC siRNA were transfected into HCT116 cells, and basal OCR and cellular ATP levels were measured. (**A**) Graph showing OCR (pM/min) over time. Data represent 3 independent experiments. $^{**}P < 0.01$. (**B**) Graph showing cellular ATP levels (RLUs) as a percentage of control in control and 2 independent clonal cell lines (clone.1 and clone.3) stably overexpressing CHCHD4.1 (myc-tagged). $^{*}P < 0.05$. Western blot analysis showing CHCHD4.1 protein expression using a myc antibody. Actin was used as a loading control. (**C**) Graph showing cellular ATP levels (RLUs) as a percentage of control in HCT116 cells transfected with CHCHD4 siRNA or a NSC siRNA. $^{*}P < 0.05$. Western blot analysis showing CHCHD4 protein knockdown. Cytochrome *c* was used as a mitochondrial control. Actin was used as a loading control.

of the HIF-1α targets CAIX and GLUT-1 (Supplemental Figure 7 and data not shown). Collectively, these data indicate that the CHCHD4 proteins regulate HIF-1α induction, angiogenesis, and tumor growth in vivo.

Increased expression of CHCHD4 enhances HIF-1α protein availability and correlates with the hypoxia gene expression signature, increased severity of tumor grade, and decreased patient survival. Since knockdown of CHCHD4 proteins blocked HIF-1α protein induction (Figure 4A), next we addressed whether CHCHD4 overexpression could enhance HIF-1α expression. Indeed, we found that CHCHD4 overexpression led to increased HIF-1α protein stability in hypoxia (Figure 6, A and B, and Supplemental Figure 8A) and significantly enhanced cellular lactate levels (Supplemental Figure 8B). Increasing evidence shows that overexpression of HIF-1α in cancer functions to drive tumor progression and metastasis (3, 32). Therefore, to investigate the clinical relevance of *CHCHD4* expression, first we analyzed gene expression microarray data from a breast cancer series that included 251 patients for whom long-term follow-up was available in at least 236 patients (33). We found that *CHCHD4* expression significantly correlated with the hypoxia gene expression signature, which was recently described (34). *CHCHD4* expression showed a significant correlation with the hypoxia score (Table 1), such that increasing *CHCHD4* expression levels were associated with a high hypoxia score (Spearman rho = 0.54, $P = 0.000001$). Next, we compared *CHCHD4* expression with tumor size as a continuous variable, and there was a highly significant correlation (Spearman rho = 0.23, $P = 0.0002$) (Supplemental Figure 9A). Similarly, increasing *CHCHD4* expression significantly correlated (Spearman rho = 0.21, $P = 0.0007$) with increasing tumor grade (Supplemental Figure 9B). Moreover, when we split the series to assess survival of patients with above or below median *CHCHD4* expression, we found that *CHCHD4* expression above the median was associated with a significantly poorer survival outcome ($P = 0.016$, log-rank test; Figure 6C). Confirming these findings, analysis of the microarray data from 3 independently published studies (35–37) showed that *CHCHD4* expression was higher in pancreatic cancer compared with that in normal pancreatic tissue (Figure 6D), and in breast cancer, increasing *CHCHD4* expression correlated with increasing tumor grade (Figure 6E). Furthermore, analyses of *CHCHD4* expression in glioma (37) showed that increasing *CHCHD4* expression correlated with increasing tumor grade (Figure 6F) and reduced survival (Figure 6G). Collectively, our

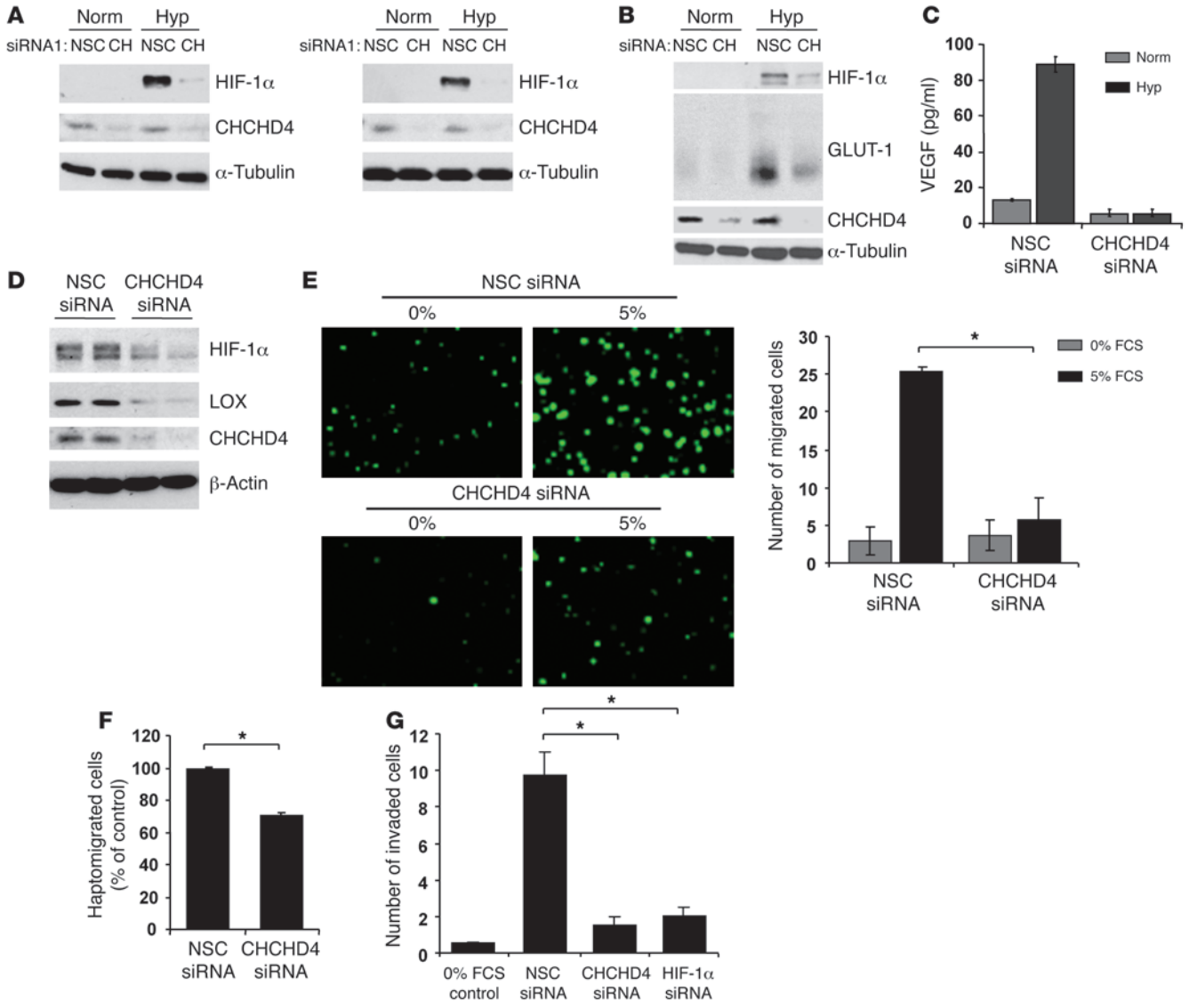

Figure 4

CHCHD4 proteins are critical for HIF-1α induction and function in response to hypoxia. (**A**) Two independent CHCHD4 siRNAs or a NSC siRNA were transfected into *p53*$^{-/-}$ HCT116 cells. Cells were incubated in normoxia (Norm) or hypoxia (1% O_2) (Hyp). Western blots showing HIF-1α and CHCHD4 proteins. Tubulin was used as a loading control. (**B**–**D**) HCT116 cells were transiently transfected with CHCHD4 siRNA or a NSC siRNA, and cells were incubated in normoxia or hypoxia (1% O_2) for 16 hours. (**B**) Western blot showing GLUT-1 protein, (**C**) graph showing VEGF (pg/ml) protein, and (**D**) Western blot showing LOX protein (hypoxia samples are shown in duplicate). (**E**–**G**) HCT116 cells transiently transfected with CHCHD4 siRNA or NSC siRNA were labeled with the fluorescence tracker CMFDA and trypsinized. Cells were (**E**) serum starved for 4 hours and assessed for their ability to migrate toward FCS (5%) as a chemoattractant using an HTS FluoroBlok insert (BD Biosciences) (original magnification, ×20), (**F**) replated and assessed for haptomigration in a scratch assay, or (**G**) replated and assessed for invasion using the BD Biosciences invasion assay system. Cells in **E**–**G** were incubated in hypoxia (1% O_2) for 16 hours then fixed and examined by microscopy. Graphs represent (**E**) the average number of migrated cells, (**F**) the percentage of haptomigrated cells, and (**G**) the average number of invaded cells. Cells were counted from at least 3 independent fields of view. *$P < 0.05$.

analyses indicate that increased expression of *CHCHD4* in human cancers significantly correlates with the gene expression signature associated with hypoxic tumors, increased severity of tumor grade, and reduced patient survival.

CHCHD4 regulates HIF-1α protein stability. Mechanisms that regulate PHD activity and VHL tumor suppressor protein–dependent HIF-1α protein stability are central to mediating changes in HIF-1α protein availability in response to hypoxia (4, 7). Changes in mitochondrial OCR at COX (complex IV) in response to hypoxia have been postulated to result in a redistribution of intracellular oxygen that leads to PHD inactivation and HIF-1α stabilization (10). To further explore the mechanism by which CHCHD4 regulates HIF-1α protein availability, we assessed the effects of loss of CHCHD4 on HIF-1α protein levels using cycloheximide (Figure 7, A and B) or the proteosome inhibitor MG132 (Figure 7C). Experiments with cycloheximide indicated that loss of CHCHD4 promoted a marked decrease in HIF-1α

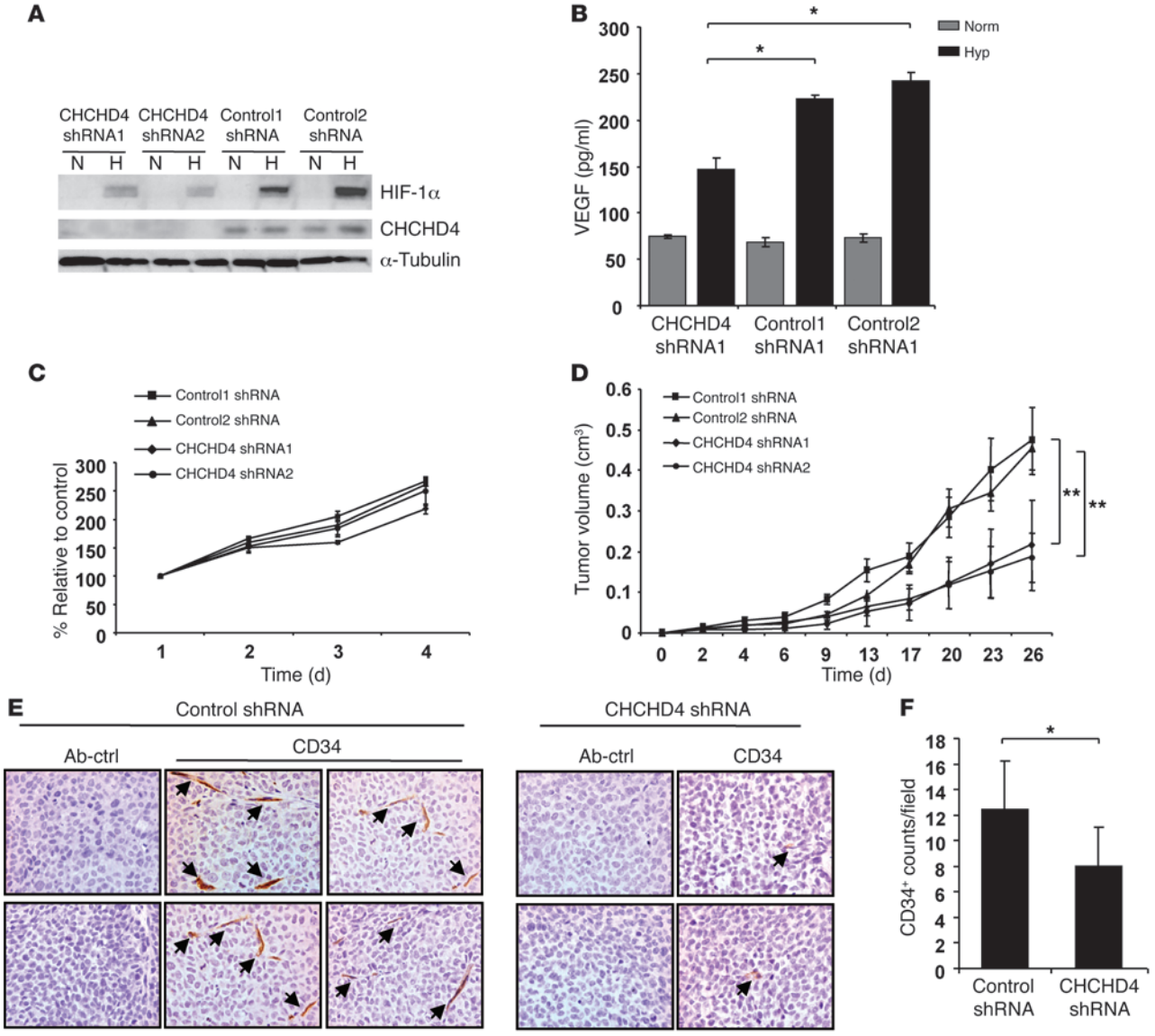

Figure 5

CHCHD4 proteins regulate tumor growth and angiogenesis in vivo. HCT116 cells stably expressing a CHCHD4 shRNA vector or 2 independent control shRNA vectors were exposed to normoxia (N) or hypoxia (H) (1% O_2) for 16 hours. Whole cell lysates were assessed (**A**) by Western blot analysis for HIF-1α and CHCHD4 protein or (**B**) by ELISA for VEGF (pg/ml) expression. *$P < 0.05$. (**C**) Graph showing cell viability (% relative to control) of HCT116 cells stably expressing 2 independent CHCHD4 shRNA vectors or 2 independent control shRNA vectors. Cell viability was measured using a MTT assay ($n = 6$; average ± SD). (**D**) HCT116 cells stably expressing 2 independent CHCHD4 shRNA or control shRNA vectors were subcutaneously injected into 8 nude mice (per group) and grown as xenografts. Graph showing tumor growth (cm^3) over time in days. Data are representative of 2 independent experiments ($n = 8$). **$P < 0.01$, for CHCHD4 shRNA1 versus control1 shRNA and CHCHD4 shRNA2 versus control2 shRNA, respectively. (**E**) Immunohistochemical analysis of HCT116 xenograft tumor sections using either an antibody control (Ab-ctrl) or CD34 staining to identify blood vessels (as indicated with arrows). (**F**) Graph shows average blood vessel ($CD34^+$) count per field of view (3 independent fields for CHCHD4 shRNA2 or control2 shRNA HCT116 xenograft tumor sections). Values are expressed as average ± SD. *$P < 0.05$.

protein half-life (Figure 7, A and B, and Supplemental Figure 10). Furthermore, we found that HIF-1α protein could rapidly accumulate in hypoxia when proteasomal degradation was blocked by MG132, even when CHCHD4 protein was knocked down (Figure 7C). Interestingly, and consistent with our findings with DFX (Supplementary Figure 1A), we found that HIF-1α stabilized by the prolyl hydroxylase inhibitor dimethyloxalylglycine (DMOG) was also not affected by CHCHD4 knockdown (Figure 7D). These data parallel previous studies with cytochrome *c*–null cells (13), in which mitochondrial ROS production induced at complex III was identified as a molecular mechanism for contributing to HIF-1α stabilization in hypoxia (11, 13). To address the role of ROS in CHCHD4-mediated enhancement of HIF-1α stabilization, we used the antioxidant *N*-acetyl cysteine. Consistent with another study (38), we found that *N*-acetyl cysteine partially blocked HIF-1α protein levels induced in hypoxia (Figure 7, E and F). However, we found that the enhanced stabilization of HIF-1α

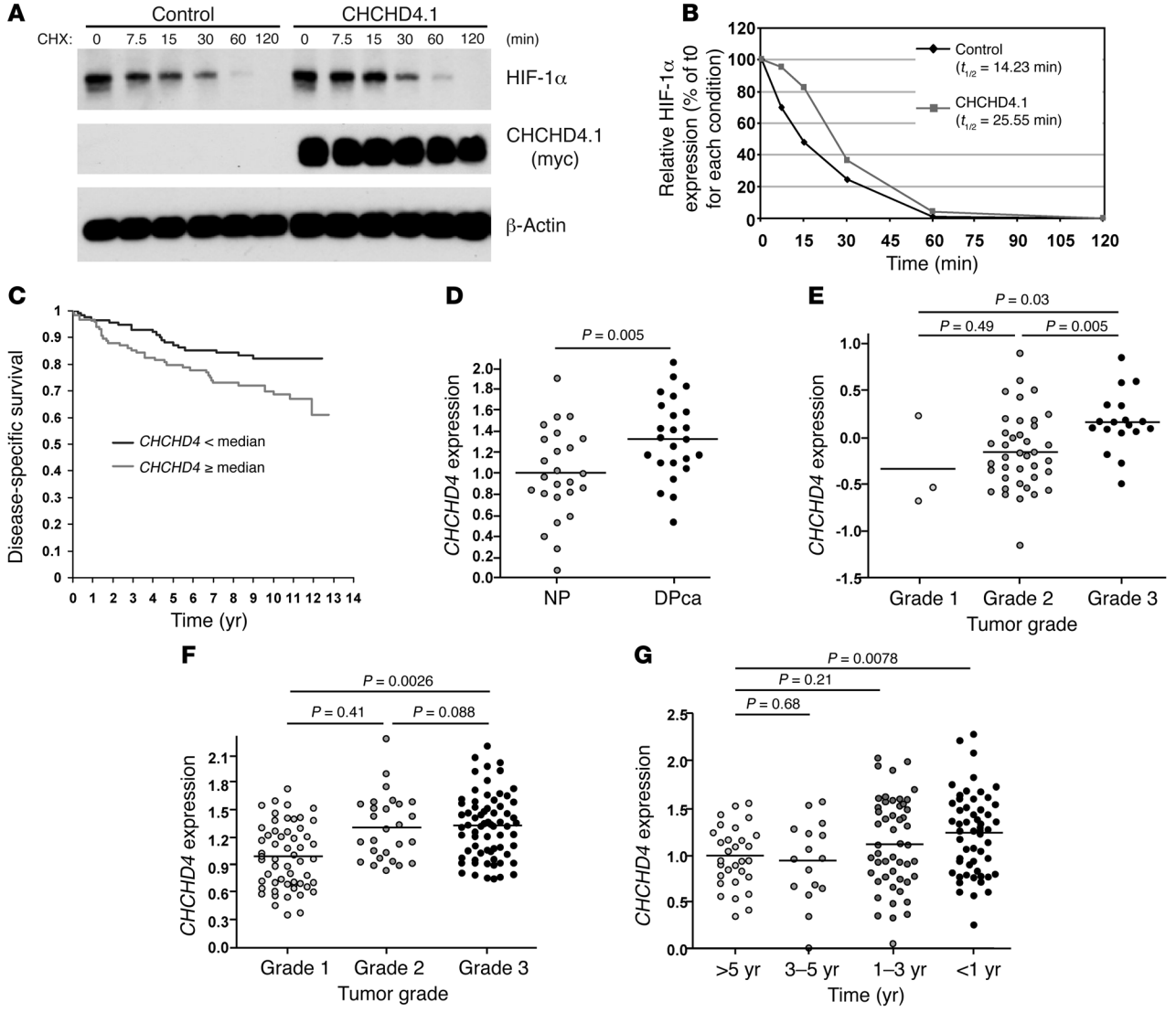

Figure 6

Increased expression of CHCHD4 enhances HIF-1α protein stability and correlates with increased severity of tumor grade and decreased patient survival. (**A** and **B**) Control HCT116 cells or HCT116 cells stably expressing myc-tagged CHCHD4.1 were exposed to hypoxia (1% O_2) for 16 hours and treated with cycloheximide (CHX; 20 μg/ml) for the times indicated. (**A**) Western blot analysis showing HIF-1α and myc-tagged CHCHD4 proteins. Actin was used as a loading control. (**B**) Graph showing HIF-1α protein levels in **A** represented as a percentage of each untreated condition (t0) measured by densitometric analysis. (**C**) Graph showing disease-specific survival over time (years) in patients with breast cancer that have associated *CHCHD4* expression below or equal to/above the median. (**D**–**G**) *CHCHD4* gene expression data were retrieved from the Oncomine website (https://www.oncomine.org/resource/login.html). Each symbol represents an individual sample. (**D**) Graph showing normalized *CHCHD4* mRNA expression in 25 normal pancreatic duct cells (NP) and 24 pancreatic ductal carcinoma samples (DPca) analyzed from gene expression profiling data described previously (35). $P = 0.005$. The bar represents the median value. (**E**) Graph showing normalized *CHCHD4* mRNA expression in grade 1, 2, and 3 breast carcinoma as indicated, analyzed from gene expression profiling data described previously (36). Significance values are indicated. The bar represents the median value. (**F** and **G**) Graphs showing (**F**) CHCHD4 DNA copy number (log_2 transformed) in grade 1, 2, and 3 glioma and (**G**) in glioma tumor samples from patients taken at survival intervals (yr) as indicated, analyzed from gene expression profiling data described previously (37). The bar represents the median value. Significance values are indicated.

protein induced by CHCHD4 overexpression in hypoxia was not sensitive to *N*-acetyl cysteine treatment (Figure 7, E and F). Therefore, finally, to ascertain whether inhibition of complex IV activity affects CHCHD4-mediated enhancement of HIF-1α protein levels in hypoxia, we blocked complex IV activity using sodium azide. We found that sodium azide blocked HIF-1α protein levels stabilized in hypoxia, even when CHCHD4 was overexpressed (Supplemental Figure 11). Taken together, our data suggest that CHCHD4 is linked to cytochrome *c* and COX (complex IV) function and are consistent with previous studies in yeast (27, 28).

Discussion

Overexpression of HIF-α occurs in many human cancers and correlates with increased hypoxia, angiogenesis and metastasis, treat-

Table 1
Increased expression of *CHCHD4* correlates with the hypoxia gene expression signature

	Gene expression signatures		
	Hypoxia	Apoptosis	Immune response
rho	0.54	0.09	0.09
P	0.000001	0.1568	0.1474
n	251	251	251

CHCHD4 gene expression data from 251 breast cancer samples (*n*) analyzed for hypoxia, apoptosis, and immune response gene signatures (rho and *P* values are indicated).

ment resistance, and poor patient survival. Targeting HIF-1α in cancer has been shown to block tumor cell growth and angiogenesis (3, 32). Thus, elucidating the key molecular mechanisms that regulate HIF-α is of particular interest therapeutically.

HIF-α is central to both sensing and responding to changes in cellular oxygen levels. However, the mechanisms by which HIF-α responds to low oxygen levels are complex. Oxygen is required for HIF-α hydroxylation catalyzed by the PHDs, which have been proposed to serve as the oxygen sensors that activate HIF-dependent gene expression (5). Intriguingly, however, HIF-1α protein accumulation does not usually occur until oxygen levels are below 5% (39), while the activities of the PHDs decrease linearly with oxygen concentration (40). Thus, other studies (8, 9, 14) propose that mitochondrial function is also important for regulating HIF-1α stabilization in hypoxia.

Here we describe and characterize functions of the human CHCHD4 proteins in the context of HIF-1α/hypoxia signaling in tumor cells. The human *CHCHD4* gene encodes 2 alternatively spliced isoforms (*CHCHD4.1* and *CHCHD4.2*) that we found to be differentially expressed across human tissues. CHCHD4.1 is identical to the mitochondrial intermembrane space (IMS) protein, MIA40 (23), which we found to be the predominant isoform detected in most human tumor cell lines that we investigated. Furthermore, we found that both CHCHD4 proteins are localized to mitochondria and are resistant to proteinase K treatment, confirming that they are not associated with the outer mitochondrial membrane. The CHCHD4 proteins contain a CPC motif and an identical evolutionarily conserved CHCH domain that bears a twin Cx_9C motif (25). Consistent with a previous study (23), we found that the cysteine residues within the CPC motif and CHCH domain are important for regulating mitochondrial localization.

The yeast Mia40 and human MIA40 proteins play a key role in the import of proteins into mitochondrial IMS (23, 30, 41). As an oxidoreductase and essential component of the DRS (41), Mia40 catalyses an oxidative protein folding mechanism, leading to the stabilization of protein conformation by the introduction of disulfide bonds into cysteine-rich proteins (24). Through this process, electrons are transferred from Mia40 via Erv1 to cytochrome *c* and COX (complex IV), thus linking the DRS to the respiratory chain (27, 28). We found that CHCHD4 proteins are important for controlling cellular OCR and ATP production. Modulation of CHCHD4 expression levels, either via knockdown or overexpression, may lead not only to changes in electron transfer via the DRS but could also change the steady-state levels of cysteine-containing proteins within the IMS, including Erv1 and Cox proteins (23). In yeast, conditions causing the reduced conformation of Mia40 also prevent its ability to import proteins into the IMS (41).

Interestingly, we found that CHCHD4 knockdown blocked HIF-1α induction and HIF-1 transcriptional activity in response to hypoxia and resulted in the inhibition of tumor cell migration, motility, and invasion. In tumor xenografts studies, we found that stable knockdown of CHCHD4 resulted in reduced HIF-1α protein levels detected in areas immediately adjacent to hypoxic regions within the tumor and led to reduced tumor growth and significantly reduced angiogenesis. Conversely, we found that overexpression of CHCHD4 in tumor cells increased HIF-1α protein stability and enhanced glycolysis. In human cancers, increased *CHCHD4* gene expression significantly correlated with the expression of a gene signature that has been shown to be associated with highly hypoxic tumors and with a range of clinical outcomes known to be associated with poor prognosis (34).

How do mitochondria interface with the cellular oxygen sensing machinery? Currently, 2 mechanisms for how mitochondria regulate HIF-1α stabilization in hypoxia have been described. First, the production of mitochondrial ROS in hypoxia at complex III (9, 11, 13) has been proposed to lead to the inhibition of PHD enzymatic activity, resulting in the stabilization of HIF-1α (15) and increased HIF-1 transcriptional activity (9). In addition, modulation of mitochondrial OCR at COX (complex IV) in response to hypoxia has been postulated to result in a redistribution of intracellular oxygen that leads to PHD inactivation and HIF-α stabilization (10) in a ROS-independent manner (10, 17–19). While these 2 mechanisms have been proposed as distinct (ROS dependent and ROS independent), the molecular basis for precisely how mitochondria regulate HIF-α/hypoxia signaling via complex III and/or COX (complex IV) is still not known.

We found that modulation of CHCHD4 expression levels affected HIF-1α protein stability. However, CHCHD4 knockdown had no significant effect on HIF-1α stabilized in normoxia by DFX or DMOG, which block the PHD enzymes. These data indicate that CHCHD4 may control the hypoxic response by mediating a regulatory effect on the PHD enzymes. Interestingly, a previous study described similar effects on HIF-1α induction using cytochrome *c*–null mouse embryonic cells (13) and highlighted a role for mitochondrial ROS in contributing to HIF-1α stabilization in hypoxia (11). Indeed, we found that treatment of cells with the antioxidant *N*-acetyl cysteine partially reduced HIF-1α protein induced in response hypoxia, as previously described (38), indicating that ROS contributes in part to HIF-1α stabilization in hypoxia. However, we found that CHCHD4-mediated enhancement of HIF-1α protein stabilized in hypoxia was not sensitive to *N*-acetyl cysteine treatment, suggesting that enhanced HIF-1α stabilization observed in hypoxia when CHCHD4 is overexpressed is not dependent on ROS. Interestingly, we found that inhibition of complex IV activity using sodium azide blocked both HIF-1α protein stabilized in hypoxia and CHCHD4-mediated enhancement of HIF-1α protein stabilized in hypoxia, indicating that human CHCHD4, like yeast Mia40, connects the DRS to cytochrome *c* and COX (complex IV) function (27, 28). Collectively, our data suggest that rather than an either/or scenario, both ROS and other mitochondrial mechanisms involving CHCHD4 potentially work in concert to contribute overall to HIF-1α stabilization in hypoxia, and it will be of interest to ascertain whether HIF-2α is also regulated in a similar manner.

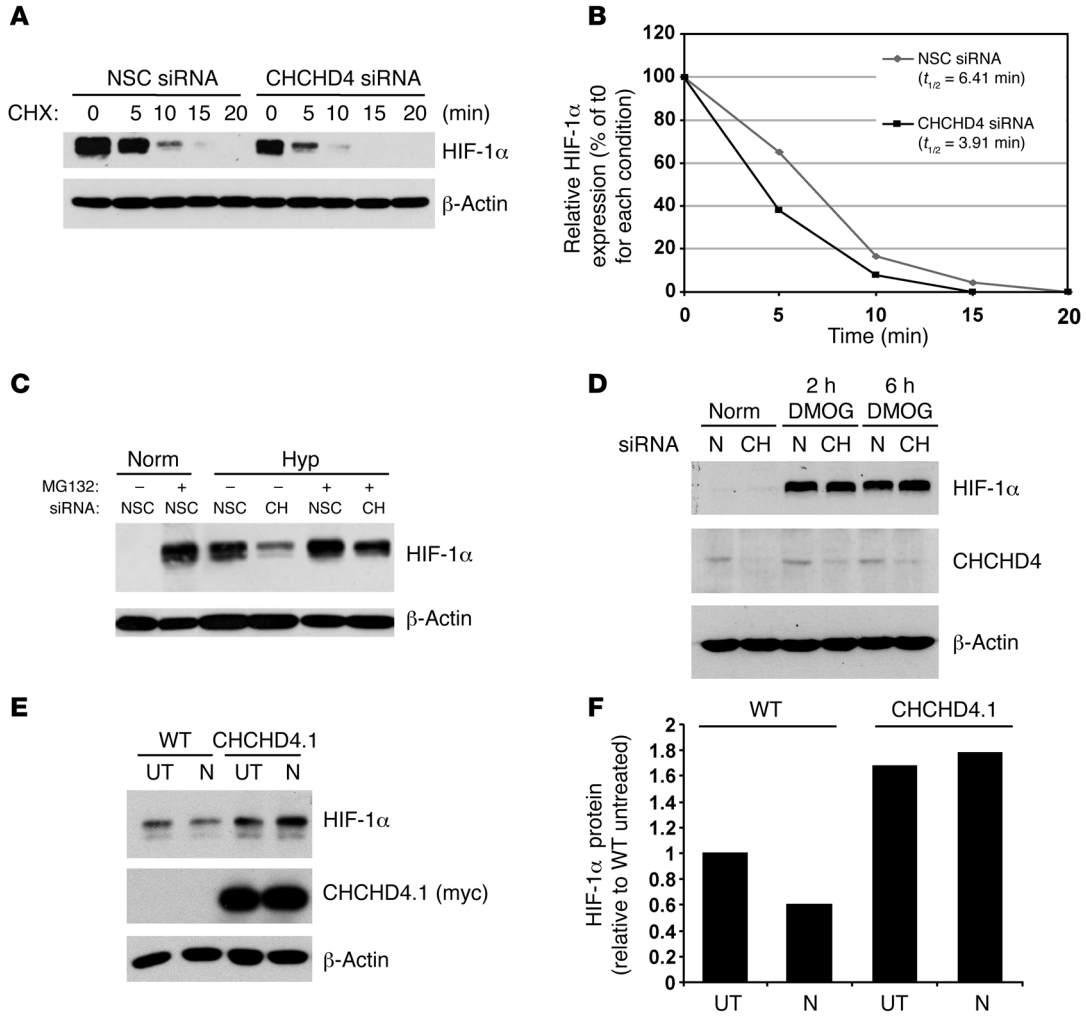

Figure 7

CHCHD4 proteins regulate HIF-1α protein stability. (**A**–**C**) HCT116 cells transiently expressing either a NSC siRNA or CHCHD4 siRNA were exposed to hypoxia (1% O_2) for 16 hours and then treated with cycloheximide (50 μg/ml) for the times indicated. Western blots were assessed for HIF-1α protein. Actin was used as a loading control. (**B**) Graph showing HIF-1α protein levels in **A** represented as a percentage of each untreated condition (t0) measured by densitometric analysis. (**C**) HCT116 cells transfected as described in **A** were exposed to MG132 (50 μM) as indicated. Western blots were assessed for HIF-1α protein. Actin was used as a loading control. (**D**) HCT116 cells transfected as described in **A** were exposed to DMOG (1 mM) for the times indicated. Western blots were assessed for HIF-1α and CHCHD4 proteins. Actin was used as a loading control. (**E** and **F**) Control HCT116 cells (WT) or HCT116 cells stably expressing myc-tagged CHCHD4.1 were exposed to hypoxia (1% O_2) for 16 hours in the absence (untreated [UT]) or presence (N) of *N*-acetyl cysteine (10 mM). (**E**) Western blots were assessed for HIF-1α and CHCHD4 proteins. Actin was used as a loading control. (**F**) Graph showing HIF-1α protein levels in **E** relative to the WT untreated samples, measured by densitometric analysis.

In summary, our study identifies a critical function for the CHCHD4 mitochondrial proteins in controlling cellular OCR, metabolism, and the HIF-1α/hypoxia response. The clinical importance of these observations is highlighted by our findings that in human tumors increased *CHCHD4* expression is associated with the hypoxia gene signature and correlates with the severity of tumor grade and poor patient survival. We propose that the CHCHD4-HIF-1α axis provides an important role in mediating metabolic adaptive responses in tumor cells.

Methods

Cell culture. Cell lines were maintained in DMEM supplemented with 10% FCS (Harlan), 100 IU/ml penicillin, 100 μg/ml streptomycin, and 2 mM glutamine (Sigma-Aldrich). The RCC4 renal carcinoma cells were purchased from the European Collection of Cell Cultures and have been described previously (7). We thank Celeste Simon (University of Pennsylvania Cancer Center, Philadelphia, Pennsylvania, USA) for providing cytochrome *c*–null mouse embryonic cells. All other cell lines were purchased from the ATCC.

Antibodies and reagents. The polyclonal antibody against CHCHD4 was generated by immunizing rabbits with GST-CHCHD4.2 fusion protein produced in *E. coli*. The antibody was affinity purified using a protein A-Sepharose bead column. Notably, endogenous CHCHD4.2 protein was usually observed to be expressed at much lower levels than CHCHD4.1 in some cell lines (e.g., HCT116 cells; Figure 1D). Interestingly, however, we found that the detection of endogenous CHCHD4.2 protein could be enriched in mitochondrial fractions (Figure 2D) when compared with that

of total lysates (Figure 1D). HIF-1α antibodies were purchased from BD Biosciences. Antibodies for β-actin and α-tubulin were purchased from Sigma-Aldrich. Anti-myc antibodies (9B11 or 9E10) were purchased from Roche and Upstate, respectively, and used in immunoprecipitation assays. The anti-myc (for localization studies), were purchased from Cell Signaling Technology. The PDI and Golgin97 antibodies for immunostaining were purchased from Invitrogen. Cellular lactate levels were measured using the Lactate Colorimetric Assay Kit (Abcam), and cellular ATP levels were measured using the CellTiter-Glo Luminescent Assay (Promega).

Sequence analysis and structural modeling. The BLAST program was used to identify similar sequences between the CHCHD4 homologs. The sequences were aligned with the ClustalW program (http://www.ebi.ac.uk/clustalw), and the CHCH domain sequence was identified using the InterProScan Sequence Search (http://www.ebi.ac.uk/InterProScan/).

siRNA duplexes, transient transfections, and shRNA lentivirus. siRNA duplexes were purchased from Dharmacon and transfected into subconfluent HCT116, Saos-2, MCF-7, RCC4, and RCC4/VHL cells using HiPerfect transfection reagent (QIAGEN) according to the manufacturer's instructions. The target sequences for CHCHD4 siRNA were 5′-ATAGCACGGAGGAGATCAA-3′ and 5′-GAGGAAACGTTGTGAATTATT-3′, corresponding to bases 546–564 and 1501–1519 in NM_144636, respectively, and targeted both *CHCHD4* isoforms. The target sequence for HIF-1α siRNA was 5′-TACGTTGTGAGTGGTATTATT-3′ from NM_001530 (1302–1322). The nonsilencing control (NSC) siRNA duplexes (5′-AATTCTCCGAACGTGTCACGT-3′) were obtained from QIAGEN. The HIF-1α siRNAs have been described by us previously (42). For stable transfection of shRNA, lentiviruses expressing a SMARTvector shRNA nontargeting control (control2), an empty vector control lentivirus (control1), or 3 independent SMARTvector shRNAs targeting *CHCHD4* (Thermo Scientific Dharmacon) were used to stably transfect HCT116 cells. Stable cells pools were selected using puromycin (0.5 μg/ml).

Basal OCR measurements. The basal OCRs of HCT116 cells were measured using a Seahorse Bioscience XF24 analyzer. Briefly, cells were seeded into 6-well plates at 2.0×10^5 cells per well 24 hours before siRNA transfection was carried out using a specific CHCHD4 siRNA or NSC siRNA using HiPerfect transfection reagent (Qiagen). Twenty-four hours later, transfection complexes were washed off, and cells were reseeded into Seahorse V7 cell culture plate at 30,000 cells per well using complete media in preparation for analysis using the Seahorse Bioscience XF24 analyzer. Prior to the assay, cells had their media changed to DMEM without sodium bicarbonate and phenol red and were placed in an incubator without CO_2. The dissolved oxygen in the media surrounding the cells was then measured, and the OCR was calculated. Mix, wait, and measure cycles of 3.0, 2.0, and 2.0 minutes, respectively, were used.

In vivo xenograft studies and study approval. For tumor growth studies, subcutaneous xenografts were established by injecting 5×10^6 cells into the right flank of 6- to 8-week-old female athymic MF1 nude mice, using 8 mice per group. Tumors were measured twice weekly until volume (length × width × height/2) reached 1.5 cm^3, and the mice were culled. Mice were given food and water ad libitum, and all experiments were in compliance with the United Kingdom Co-ordinating Committee on Cancer Research (UKCCCR) Guidelines for the Welfare of Animals in Experimental Neoplasia. Tumor preparation and microscopy were carried out as described previously (43). All in vivo studies were performed in accordance with the United Kingdom Home Office Animal Procedures Act of 1986 and with approval of the University College London Animal Ethics Committee.

CHCHD4 gene expression analyses. To investigate the CHCHD4 expression relative to that of other patterns of gene expression, we analyzed a breast cancer series in which U133A and B Affymetrix chips had been used (33). Information on up to 251 breast cancer samples was analyzed where long-term patient follow-up was also available (33). We compared CHCHD4 expression with a hypoxia profile that we have previously described (34). This showed a clear correlation (Spearman rho = 0.54, $P = 0.00001$) with the hypoxia score. The gene expression data were retrieved from the Gene Expression Omnibus (GEO) website (http://www.ncbi.nlm.nih.gov/geo/). SPPS and R were used for statistical calculations. Independent *CHCHD4* gene expression data were also retrieved from the Oncomine website (https://www.oncomine.org/resource/login.html). The Prism program was used for statistical calculations, and graphic values represent normalized *CHCHD4* mRNA expression and CHCHD4 DNA copy number (log_2 transformed) as indicated. The study from Ishikawa et al. includes 25 normal pancreatic duct cells and 24 pancreatic ductal carcinoma samples (GEO accession no. GSE1542) (35). Gene expression profiling was performed using the Affymetrix Human Genome U133A and U133B. The study from Ma et al. includes 3 breast carcinomas with grade 1 classification, 39 breast carcinomas with grade 2 classification, and 18 breast carcinomas with grade 3 classification (GEO accession no. GSE1378) (36). A custom-designed 22,000-gene oligonucleotide (60-mer) microarray was fabricated (Agilent Technologies) for gene expression profiling. The study from Kotliarov et al. for tumor grade includes 55 gliomas with grade 1 classification, 41 gliomas with grade 2 classification, 82 gliomas with grade 3 classification (GEO accession no. GSE6109) (37). The survival study includes 30 gliomas from patients with more than 5-year survival, 16 gliomas from patients with 3- to 5-year survival, 50 gliomas from patients with 1- to 3-year survival, and 53 gliomas from patients with less than 1-year survival. The Genechip Human Mapping 100K arrays (Affymetrix), which covers 116,204 single nucleotide polymorphism loci in the human genome, with a mean intermarker distance of 23.6 kb, was used to study the DNA copy number.

Statistics. All in vitro experiments are representative of at least 3 independent repeats. The numbers of mice or tissues used in each experiment are presented in the text or figure legends. Values are expressed as mean ± SEM unless otherwise stated, and statistical significance was determined by a 1-tailed or 2-tailed Student's *t* test, with significance set at $P < 0.05$.

Acknowledgments

Thanks to William Kaelin Jr. (Harvard Medical School, Boston, USA) and Navdeep Chandel (Northwestern Medical School, Chicago, USA) for helpful discussions, and Neville Ashcroft for database analyses. We thank George Chennell for technical assistance with oxygen consumption measurements (University College London), and Ali Tavassoli and Ida K. Nordgren (University of Southampton, Southampton, United Kingdom) for their initial input. J. Yang, O. Staples, L.W. Thomas, E. Poon, and A. Ahmed were funded by Cancer Research UK grants C7358/A4420, C7358/A11223, C7358/A9958, and C7358/A8020. M. Robson, B.R. Pedley, and E. El-Emir were funded by Cancer Research UK grant C34/A5149, European Union Project ADAMANT (HEALT-F2-2008-201342), King's College London, and University College London Comprehensive Cancer Imaging Centre, Cancer Research UK, and Engineering and Physical Sciences Research Council, in association with the MRC and Department of Health (England).

Received for publication May 2, 2011, and accepted in revised form November 16, 2011.

Address correspondence to: Margaret Ashcroft, Centre for Cell Signalling and Molecular Genetics, University College London, London, United Kingdom. Phone: 44.0.20.7679.6205; Fax: 44.0.20.7679.6211; E-mail: m.ashcroft@ucl.ac.uk.

Jun Yang's present address is: St. Jude Children's Research Hospital, Memphis, Tennessee, USA.

1. Kaelin WG Jr, Ratcliffe PJ. Oxygen sensing by metazoans: the central role of the HIF hydroxylase pathway. *Mol Cell*. 2008;30(4):393–402.
2. Wang GL, Jiang BH, Rue EA, Semenza GL. Hypoxia-inducible factor 1 is a basic-helix-loop-helix-PAS heterodimer regulated by cellular O2 tension. *Proc Natl Acad Sci U S A*. 1995;92(12):5510–5514.
3. Poon E, Harris AL, Ashcroft M. Targeting the hypoxia-inducible factor (HIF) pathway in cancer. *Expert Rev Mol Med*. 2009;11:e26.
4. Ivan M, et al. HIFalpha targeted for VHL-mediated destruction by proline hydroxylation: implications for O2 sensing. *Science*. 2001;292(5516):464–468.
5. Jaakkola P, et al. Targeting of HIF-alpha to the von Hippel-Lindau ubiquitylation complex by O2-regulated prolyl hydroxylation. *Science*. 2001; 292(5516):468–472.
6. Yu F, White SB, Zhao Q, Lee FS. HIF-1alpha binding to VHL is regulated by stimulus-sensitive proline hydroxylation. *Proc Natl Acad Sci U S A*. 2001; 98(17):9630–9635.
7. Maxwell PH, et al. The tumour suppressor protein VHL targets hypoxia-inducible factors for oxygen-dependent proteolysis. *Nature*. 1999; 399(6733):271–275.
8. Agani FH, Pichiule P, Chavez JC, LaManna JC. The role of mitochondria in the regulation of hypoxia-inducible factor 1 expression during hypoxia. *J Biol Chem*. 2000;275(46):35863–35867.
9. Chandel NS, et al. Reactive oxygen species generated at mitochondrial complex III stabilize hypoxia-inducible factor-1alpha during hypoxia: a mechanism of O2 sensing. *J Biol Chem*. 2000; 275(33):25130–25138.
10. Hagen T, Taylor CT, Lam F, Moncada S. Redistribution of intracellular oxygen in hypoxia by nitric oxide: effect on HIF1alpha. *Science*. 2003; 302(5652):1975–1978.
11. Guzy RD, et al. Mitochondrial complex III is required for hypoxia-induced ROS production and cellular oxygen sensing. *Cell Metab*. 2005;1(6):401–408.
12. Lin X, et al. A chemical genomics screen highlights the essential role of mitochondria in HIF-1 regulation. *Proc Natl Acad Sci U S A*. 2008;105(1):174–179.
13. Mansfield KD, et al. Mitochondrial dysfunction resulting from loss of cytochrome c impairs cellular oxygen sensing and hypoxic HIF-alpha activation. *Cell Metab*. 2005;1(6):393–399.
14. Chandel NS, Maltepe E, Goldwasser E, Mathieu CE, Simon MC, Schumacker PT. Mitochondrial reactive oxygen species trigger hypoxia-induced transcription. *Proc Natl Acad Sci U S A*. 1998;95(20):11715–11720.
15. Pan Y, et al. Multiple factors affecting cellular redox status and energy metabolism modulate hypoxia-inducible factor prolyl hydroxylase activity in vivo and in vitro. *Mol Cell Biol*. 2007;27(3):912–925.
16. Agani FH, Pichiule P, Carlos Chavez J, LaManna JC. Inhibitors of mitochondrial complex I attenuate the accumulation of hypoxia-inducible factor-1 during hypoxia in Hep3B cells. *Comp Biochem Physiol A Mol Integr Physiol*. 2002;132(1):107–109.
17. Brown ST, Nurse CA. Induction of HIF-2alpha is dependent on mitochondrial O2 consumption in an O2-sensitive adrenomedullary chromaffin cell line. *Am J Physiol Cell Physiol*. 2008;294(6):C1305–C1312.
18. Doege K, Heine S, Jensen I, Jelkmann W, Metzen E. Inhibition of mitochondrial respiration elevates oxygen concentration but leaves regulation of hypoxia-inducible factor (HIF) intact. *Blood*. 2005; 106(7):2311–2317.
19. Chua YL, et al. Stabilization of hypoxia-inducible factor-1alpha protein in hypoxia occurs independently of mitochondrial reactive oxygen species production. *J Biol Chem*. 2010;285(41):31277–31284.
20. Eisenberg D, Marcotte EM, Xenarios I, Yeates TO. Protein function in the post-genomic era. *Nature*. 2000;405(6788):823–826.
21. Date SV. Estimating protein function using protein-protein relationships. *Methods Mol Biol*. 2007; 408:109–127.
22. Date SV. The Rosetta stone method. *Methods Mol Biol*. 2008;453:169–180.
23. Hofmann S, Rothbauer U, Muhlenbein N, Baiker K, Hell K, Bauer MF. Functional and mutational characterization of human MIA40 acting during import into the mitochondrial intermembrane space. *J Mol Biol*. 2005;353(3):517–528.
24. Banci L, et al. MIA40 is an oxidoreductase that catalyzes oxidative protein folding in mitochondria. *Nat Struct Mol Biol*. 2009;16(2):198–206.
25. Longen S, et al. Systematic analysis of the twin cx(9)c protein family. *J Mol Biol*. 2009;393(2):356–368.
26. Hetz C, et al. Proapoptotic BAX and BAK modulate the unfolded protein response by a direct interaction with IRE1alpha. *Science*. 2006;312(5773):572–576.
27. Bihlmaier K, Mesecke N, Terziyska N, Bien M, Hell K, Herrmann JM. The disulfide relay system of mitochondria is connected to the respiratory chain. *J Cell Biol*. 2007;179(3):389–395.
28. Bien M, Longen S, Wagener N, Chwalla I, Herrmann JM, Riemer J. Mitochondrial disulfide bond formation is driven by intersubunit electron transfer in Erv1 and proofread by glutathione. *Mol Cell*. 2010;37(4):516–528.
29. Fukuda R, Zhang H, Kim JW, Shimoda L, Dang CV, Semenza GL. HIF-1 regulates cytochrome oxidase subunits to optimize efficiency of respiration in hypoxic cells. *Cell*. 2007;129(1):111–122.
30. Chacinska A, et al. Essential role of Mia40 in import and assembly of mitochondrial intermembrane space proteins. *Embo J*. 2004;23(19):3735–3746.
31. Terziyska N, et al. Mia40, a novel factor for protein import into the intermembrane space of mitochondria is able to bind metal ions. *FEBS Lett*. 2005;579(1):179–184.
32. Semenza GL. Defining the role of hypoxia-inducible factor 1 in cancer biology and therapeutics. *Oncogene*. 2010;29(5):625–634.
33. Miller LD, et al. An expression signature for p53 status in human breast cancer predicts mutation status, transcriptional effects, and patient survival. *Proc Natl Acad Sci U S A*. 2005;102(38):13550–13555.
34. Winter SC, et al. Relation of a hypoxia metagene derived from head and neck cancer to prognosis of multiple cancers. *Cancer Res*. 2007;67(7):3441–3449.
35. Ishikawa M, et al. Experimental trial for diagnosis of pancreatic ductal carcinoma based on gene expression profiles of pancreatic ductal cells. *Cancer Sci*. 2005;96(7):387–393.
36. Ma XJ, et al. A two-gene expression ratio predicts clinical outcome in breast cancer patients treated with tamoxifen. *Cancer Cell*. 2004;5(6):607–616.
37. Kotliarov Y, et al. High-resolution global genomic survey of 178 gliomas reveals novel regions of copy number alteration and allelic imbalances. *Cancer Res*. 2006;66(19):9428–9436.
38. Gao P, et al. HIF-dependent antitumorigenic effect of antioxidants in vivo. *Cancer Cell*. 2007;12(3):230–238.
39. Jiang BH, Semenza GL, Bauer C, Marti HH. Hypoxia-inducible factor 1 levels vary exponentially over a physiologically relevant range of O2 tension. *Am J Physiol*. 1996;271(4 pt 1):C1172–C1180.
40. Hirsila M, Koivunen P, Gunzler V, Kivirikko KI, Myllyharju J. Characterization of the human prolyl 4-hydroxylases that modify the hypoxia-inducible factor. *J Biol Chem*. 2003;278(33):30772–30780.
41. Mesecke N, et al. A disulfide relay system in the intermembrane space of mitochondria that mediates protein import. *Cell*. 2005;121(7):1059–1069.
42. Carroll VA, Ashcroft M. Role of hypoxia-inducible factor (HIF)-1alpha versus HIF-2alpha in the regulation of HIF target genes in response to hypoxia, insulin-like growth factor-I, or loss of von Hippel-Lindau function: implications for targeting the HIF pathway. *Cancer Res*. 2006;66(12):6264–6270.
43. El Emir E, et al. Predicting response to radioimmunotherapy from the tumor microenvironment of colorectal carcinomas. *Cancer Res*. 2007; 67(24):11896–11905.